

Cooperative Coupling of Cyanine and Tictoid Twisted π -Systems to Amplify Organic Chromophore Cubic Nonlinearities

Yanrong Shi,[†] Alexander J.-T. Lou,[†] Guang S. He,[‡] Alexander Baev,[‡] Mark T. Swihart,[§] Paras N. Prasad,^{*,‡,||} and Tobin J. Marks^{*,†}

[†]Department of Chemistry and the Materials Research Center, Northwestern University, Evanston, Illinois 60208, United States

[‡]The Institute for Lasers, Photonics and Biophotonics, State University of New York at Buffalo, Buffalo, New York 14260, United States

[§]Department of Chemical and Biological Engineering, State University of New York at Buffalo, Buffalo, New York 14260, United States

^{||}Department of Chemistry, Korea University, Seoul 136-701, Korea

Supporting Information

ABSTRACT: We report a new class of hybrid π -electron chromophores with a large, sign-tunable third-order nonlinear optical (NLO) response, achieved via cooperative coupling of cyanine dye bond-length alternation effects with the rich density of states in zwitterionic twisted π -system chromophores. A combined synthetic, linear/nonlinear spectroscopic, and quantum chemical study reveals exceptional third-order response exceeding the sum of the individual chromophore contributions.

Interest in organic third-order nonlinear optical (NLO) materials has grown dramatically in recent years due to their promise in optical telecommunications, ultrahigh speed signal processing, real-time target recognition, and aberration-corrected imaging, where linear and nonlinear absorption must be minimized, and in optical power limiting (OPL), where nonlinear absorption must be maximized.¹ Target figures of merit for all-optical signal processing are $W \equiv n_2 I / (\alpha_1 \lambda) \gg 1$ and $T \equiv \alpha_2 \lambda / n_2 \ll 1$. Therefore, high-performance materials are only possible if losses are balanced against the nonlinearity. The quantity governing intense light propagation in centrosymmetric media is frequency-dependent third-order NLO susceptibility, which in the case of single beam propagation is $\chi^{(3)}(-\omega; \omega, -\omega, \omega)$, where ω is the input beam frequency. In general, $\chi^{(3)}(-\omega; \omega, -\omega, \omega)$ is complex; the imaginary part determines the nonlinear attenuation of high-intensity light, leading to two-photon absorption and the hyper-Raman effect. Enhanced $\text{Im}\{\chi^{(3)}\}$ materials are useful for eye and sensor protection from high-intensity lasers by OPL and have been receiving attention for two decades.² In contrast, nonresonant $\text{Re}\{\chi^{(3)}\}$ materials are beneficial for optical parametric oscillation, frequency up-conversion, and intensity-dependent refractive index modulation, all important applications in which the input light intensity loss due to one- and/or two-photon absorption must be minimized.³

Macroscopic third-order optical susceptibility, $\chi^{(3)}(-\omega; \omega, -\omega, \omega)$, is related to microscopic (molecular) second hyperpolarizability, $\gamma(-\omega; \omega, -\omega, \omega)$, via eq 1, where N is the molecular number density and $L(\omega)$ is a local field factor

describing the net effective field experienced by the chromophore.⁴ $\chi^{(3)}$ material design involves rationally optimizing all three terms by manipulating electronic, geometrical, and bulk structural characteristics. The simplest γ description

$$\chi^{(3)}(-\omega; \omega, -\omega, \omega) = NL^4(\omega)\gamma(-\omega; \omega, -\omega, \omega) \quad (1)$$

uses a three-level model [eq 2]⁵

$$\gamma \propto -\frac{\mu_{eg}^4}{E_{eg}^3} + \frac{\mu_{e'e}^2 \mu_{eg}^2}{E_{eg}^2 E_{e'g}} + \frac{\mu_{eg}^2 (\mu_{ee} - \mu_{gg})}{E_{eg}^3} \quad (2)$$

where μ_{ij} and μ_{ii} are the transition and permanent dipole moments, respectively, and E_{ij} is the transition energy.

Past γ enhancement approaches used one- (1-D) and two-dimensional (2-D) π -system extension and tuning bond length alternation (BLA) via affecting intramolecular charge transfer and engineering multipolar charge distributions. BLA can be used to maximize γ via solvent polarity or donor/acceptor substituents.⁶ Although such strategies are promising, they are not yet practical because: (i) increasing π -conjugation length is limited by γ saturation effects with the number of double bonds; (ii) increasing π -delocalization may compress the highest occupied molecular orbital–lowest unoccupied molecular orbital (HOMO–LUMO) gap, creating one- and/or multiphoton absorption losses at $\chi^{(3)}$ application wavelengths; (iii) increasing conjugation length often compromises chemical, thermal, and/or photochemical stability; and (iv) BLA trends can break down in polar matrices.⁷

We recently pursued a radically different approach to enhance γ , namely, twisted π -systems,⁸ and showed that chromophore TMC-2 (Figure 1), despite its relatively compact size and conjugation length, exhibits a greater third-order NLO response than many planar dyes of comparable or greater π -expanse.⁹ Closely spaced TMC-2 zwitterionic states greatly reduce the denominator energy terms [eq 2], substantially enhancing the second- and third-order NLO response. In TMC-2, twisting is enforced by tetra-*o*-methylbiaryl fragments joined via Buchwald–Suzuki coupling,¹⁰ which typically

Received: January 30, 2015

Published: March 26, 2015



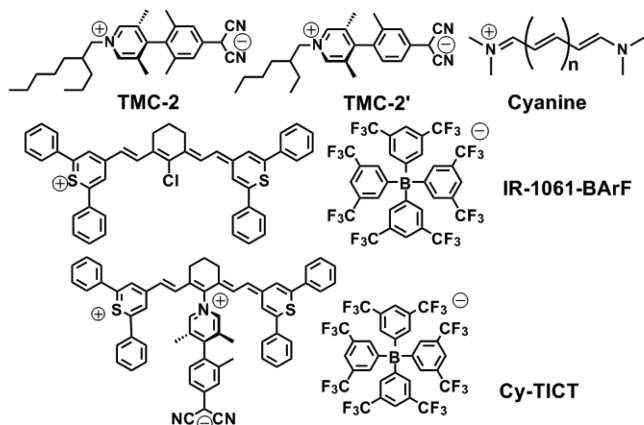


Figure 1. Structures of twisted/tictoid chromophores TMC-2 and TMC-2', a generic cyanine dye, dye IR-1061-BArF, and new hybrid chromophore Cy-TICT.

proceeds in low yields, likely reflecting steric constraints. Guided by quantum chemical computations, we pursued an alternative, more efficient approach that provides comparable π -twisting and NLO responses by introducing a tris-*o*-methylbiaryl fragment (TMC-2', Figure 1). Contemporaneously, cyanine-like dyes (Figure 1) with favorable BLA and narrow electronic absorption bands were shown to exhibit large γ and reduced linear absorption at the 1550 nm telecommunication wavelength.¹¹

Here, we report a heretofore unexplored strategy of coupling BLA with closely spaced, twisted π -system zwitterionic states that minimize the denominators in eq 1 and find marked cooperative amplification of cubic nonlinearity, namely, the second hyperpolarizability (macroscopic n_2) of the hybrid system is not a simple sum of those of the parent individual cyanine dye and twisted tictoid chromophore. We report the synthesis and third-order response of the first of a new class of hybrid chromophores with third-order properties substantially exceeding those of the parent chromophores, Cy-TICT (Figure 1). Theoretical analysis shows that hybridization and increased state densities in Cy-TICT, together with favorable changes in cyanine BLA, are critical to enhancing the nonlinearity. All γ measurements and computations can be performed at telecommunication wavelengths due to the very low linear optical absorption.

Cy-TICT synthesis begins by displacing Cl^- at the cyclohexylene juncture of ion-exchanged dye IR-1061 (see Scheme S1 in the Supporting Information (SI)). The twisted building block is prepared in good yield, as it is for TMC-2,^{8a} but with a tris-*o*-methylbiaryl fragment to enforce twisting. Both experimental and theoretical data support the assigned structure. Comparison of TMC-2 and TMC-2' in the solid state and in solution using X-ray diffraction, optical spectroscopy, and density functional theory (DFT) calculations indicate structural similarities overall with a dihedral twist near 90° . For Cy-TICT, 1-D/2-D heteronuclear single quantum coherence (HSQC), correlation spectroscopy (COSY), nuclear Overhauser effect NMR spectroscopy (NOESY), elemental analysis, and large solvatochromic shifts observed in the linear optical spectra (Figure 2) confirm the linking of the twisted moiety to the near-planar cyanine (see SI for details).¹²

IR-1061-BArF and Cy-TICT linear optical properties were first characterized in solvents of varying dielectric constant. Both dyes are stable in CH_2Cl_2 and CH_3CN , exhibiting no

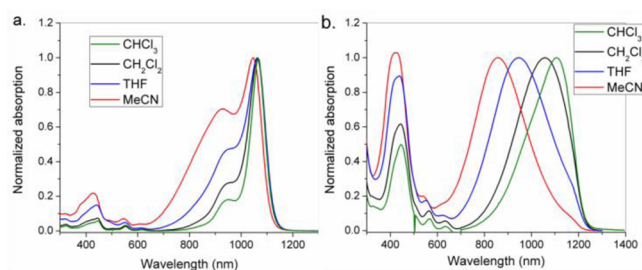


Figure 2. Solution optical absorption spectra of (a) IR-1061-BArF and (b) Cy-TICT in the indicated solvents.

detectable change in spectra in ambient conditions over two days. Typical of most cyanine dyes,¹¹ the linear IR-1061-BArF optical spectra exhibit slight positive shifts in polar solvents (Figure 2a) with broadening of the principal band and an increase in the shorter wavelength shoulder in more polar solvents. In marked contrast, Cy-TICT exhibits very large negative solvatochromic shifts, ~ 250 nm upon going from CH_3CN to CH_2Cl_2 (Figure 2b), indicative of a twisted π -system zwitterionic ground state.⁸ Whereas the peak IR-1061-BArF extinction coefficients are very large ($>10^5 \text{ M}^{-1} \text{ cm}^{-1}$) in both solvents, typical of cyanines, the Cy-TICT absorption is significantly weaker and broader in both solvents and is in no way explicable as a simple superposition of the TMC-2' and IR-1061-BArF spectra. Furthermore, the Cy-TICT spectrum in CH_2Cl_2 is independent of concentration over a 23-fold range (Figure S5 in the SI). The ground state to first excited electronic state transition dipole moments, calculated from the IR-1061-BArF spectra, are 16.9 and 18.7 D in CH_3CN and CH_2Cl_2 , respectively, and are larger than those of Cy-TICT at 10.5 and 12.1 D, respectively. Thus, twisted chromophore incorporation significantly alters the parent cyanine dye electronic states, as confirmed by the theoretical analysis below.

Large third-order response is invariably accompanied by resonance enhancement, usually one- or two-photon,^{1c} with the response dependent on the input wavelength. Z-scan results for Cy-TICT/ CH_2Cl_2 at 1305 and 1410 nm are presented in the SI (Figures S6 and S7). Note that both the Cy-TICT/ CH_2Cl_2 -induced refractive index change and the nonlinear absorption decrease with increasing input wavelength, indicating resonance enhancement. In contrast, quartz exhibits a constant non-resonant, nonlinear refractive index (n_2) value = $3 \times 10^{-16} \text{ cm}^2/\text{W}$ from 600 to 1600 nm.¹³ The Cy-TICT/ CH_3CN Z-scan shows a significantly lower nonlinearity, indicating a solvent-dependent response (Figure S8 in the SI). Furthermore, comparing these results to the IR-1061-BArF/ CH_2Cl_2 Z-scan data indicates that for the same solvent and wavelength the Cy-TICT nonlinear refractive index and nonlinear absorption are significantly greater than those of IR-1061-BArF (Figure S9 in the SI).

Figure 3a shows open-aperture Z-scan results for 0.01 M Cy-TICT/ CH_2Cl_2 at 1305 nm; the dashed line is the best fit to a saturable two-photon absorption (2PA) model.¹⁴ Figure 3b shows nonlinear transmittance as a function of input pulse intensity, and the best-fit curve clearly indicates optical power limiting behavior. Table I summarizes the third-order parameters of the present chromophores. At ~ 1300 nm, Cy-TICT/ CH_2Cl_2 exhibits both a larger refractive index change and greater nonlinear absorptivity than does IR-1061-BArF; the former property enables optical switching, and the latter enables optical power limiting. Comparing the Cy-TICT third-

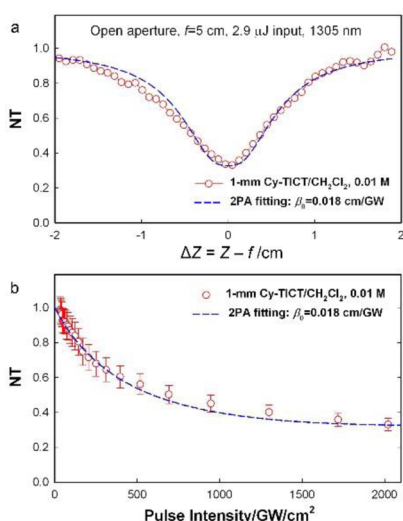


Figure 3. (a) Open-aperture Z-scan (nonlinear transmittance, $f = 5$ cm) using ~ 160 fs $2.9 \mu\text{J}$ laser pulses at 1305 nm for Cy-TICT/ CH_2Cl_2 . (b) Nonlinear transmittance as a function of input pulse intensity, showing optical power limiting. Solid curve is the best fit to two-photon absorption (2PA) theory.

Table I. Third-Order NLO Parameters for Chromophores from Z-Scan Measurements in Solution^a

	Cy-TICT (CH_2Cl_2)		Cy-TICT (CH_3CN)	IR1061-BArF (CH_2Cl_2)
	1305 nm	1410 nm	1305 nm	1305 nm
contribution to n_2 at 0.01 M ($10^{-6} \text{ cm}^2/\text{GW}$)	-2.04	-0.72	-1.11	-1.20
contribution to Re. $\chi^{(3)}$ at 0.01 M (10^{-14} esu)	-3.88	-1.37	-2.11	-2.28
Re. γ (10^{-33} esu)	-6.43	-2.27	-3.50	-3.78
2PA coefficient β (cm/GW)	0.018	0.0045	0.0033	0.0053
2PA cross-section (GM)	45.5	10.6	8.34	13.4
contribution to Im. $\chi^{(3)}$ at 0.01 M (10^{-15} esu)	3.54	0.953	0.649	1.04
Im. γ (10^{-35} esu)	58.8	15.8	10.8	17.3
linear transmittance (for 1 mm solution)	~ 0.70	~ 0.95	~ 0.75	~ 0.90
T parameter	1.1515	0.8813	0.388	0.5764

^aExperimental uncertainty = $\pm 10\%$.

order nonlinearity parameters with those of TMC-2 reported earlier⁹ and IR-1061-BArF (Table II) clearly shows marked synergistic effects of combining the twist and cyanine fragments.

Table II. Comparison of Cy-TICT, IR-1061-BArF, and TMC-2 NLO Parameters

	Cy-TICT (1305 nm)	IR1061-BArF (1305 nm)	TMC-2 ⁹ (1172 nm)
contribution to n_2 at 0.01 M ($10^{-6} \text{ cm}^2/\text{GW}$)	-2.04	-1.20	0.15
Re. γ (10^{-33} esu)	-6.43	-3.78	0.50
2PA cross-section (GM)	45.50	13.40	1.50
Im. γ (10^{-35} esu)	58.80	17.30	<1.30
linear transmittance	0.77	0.98	0.98

For a better understanding of the twist motif influence on the Cy-TICT NLO response, the linear absorption, two-photon absorption, real part of Cy-TICT second hyperpolarizability, and that of IR-1061-BArF were computed as a function of (cyanine)C–N(pyridinium) and (pyridinium)C–C(aryl) torsion.^{8b,15} Computation of γ and the all-optical switching parameters T and W^9 was performed with DFT at the CAM-B3LYP/3-21G level for Cy-TICT and compared to those of IR-1061-BArF (Table III). Note that Cy-TICT in vacuo near 90° (pyridinium)C–C(aryl) twist geometry and IR-1061-BArF show the same γ signs and dispersions, and that the sign of n_2 at 1300 nm and the gradient (anomalous dispersion) agree with the experimental data (Table I). The magnitude of γ for Cy-TICT with an enforced twist near 90° reproduces the experimental trend versus IR-1061-BArF, consistent with an $\sim 90^\circ$ Cy-TICT twist geometry in solution. Note that DFT is known to underestimate excitation energies, even with long-range corrected functionals (e.g., CAM-B3LYP here); thus, wavelengths of interest must be red-shifted by up to ~ 100 nm, depending on the solvent, to obtain more accurate n_2 and γ values. Indeed, dispersion effects for a wavelength red shift will lower γ for Cy-TICT and IR-1061-BArF, bringing it closer to the experimental values. In summary, Cy-TICT with an enforced primary twist exhibits the greatest all-optical switching performance at 1305 nm, reflecting a large absolute γ value and relatively low nonresonant two-photon absorption (Table III). Cy-TICT has a γ that is much larger than TMC-2,⁹ and the computed 1350 nm two-photon absorption cross-section, σ_2 , at an $\sim 90^\circ$ twist angle is exceptionally large, reaching 3364 GM, making Cy-TICT an intriguing candidate for optical limiting applications.

To analyze coupling between the Cy-TICT zwitterionic and cyanine states, three sets of MOs were computed for Cy-TICT (Figure 4), TMC-2', and IR-1061-BArF (Figure S10 in the SI). Note that Cy-TICT is clearly a hybrid of the parent chromophore orbital compositions with multiple transitions (cross-couplings) between, for example, the TMC-2' HOMO and the IR-1061-BArF LUMO and LUMO+1. Such cross-couplings result in strong transition dipole moments between states and, thus, in cooperative enhancement of the Cy-TICT γ . The IR-1061-BArF and Cy-TICT linear absorption spectra (Figure 2) confirm this significant cross-coupling. Furthermore, the increased density of states also contributes to γ enhancement. Orbital hybridization results in spectral shifts of the resonances, so there is an exciting opportunity here to manipulate the sign of n_2 at selected wavelengths (see Table III). The BLA parameters for the optimized structures in vacuum decrease from 0.097 for IR-1061 to 0.086 for Cy-TICT, whereas optimization in CHCl_3 yields 0.1073 for IR-1061 and 0.0957 for Cy-TICT. Cyanines with small BLAs are known to yield large γ values, maximizing γ at BLA = 0 (the cyanine limit).^{6,7,11,16} The small decrease in the calculated BLA parameter for the Cy-TICT structure versus the pure cyanine IR-1061 may also contribute to the observed enhanced γ . To confirm the central role of the twist motif in the cooperative enhancement of the Cy-TICT system nonlinearity, we introduced a simple pyridine molecule at the central cyanine position of IR-1061 and computed the second hyperpolarizability. The computational analysis indicates that pyridine introduction has a minimal effect (Table SIII and Figure S11 in the SI), confirming our structure nonlinearity model (see SI for more details).

Table III. Second Hyperpolarizabilities ($\text{Re}\{\gamma_{\text{av}}\}$) Computed at the CAM-B3LYP/3-21G Level of Theory

	$\gamma_{\text{av}} 10^5 \text{ au}$ (1300 nm)	$\gamma_{\text{av}} 10^5 \text{ au}$ (1550 nm)	$\gamma_{\text{av}} 10^{-33} \text{ esu}$ (1300 nm)	$\gamma_{\text{av}} 10^{-33} \text{ esu}$ (1550 nm)	T/W (1300 nm)	T/W (1550 nm)
Cy-TICT-BArF ⁻ (vacuum)	-15365	430	-774	22	0.62/84.4	19.9/2.86
Cy-TICT-BArF ⁻ , 90° twist	-100000	449	-5037	23	0.07/1276	17.48/360
IR-1061-BArF	-54835	192	-2762	10	0.14/297	32.1/1.44

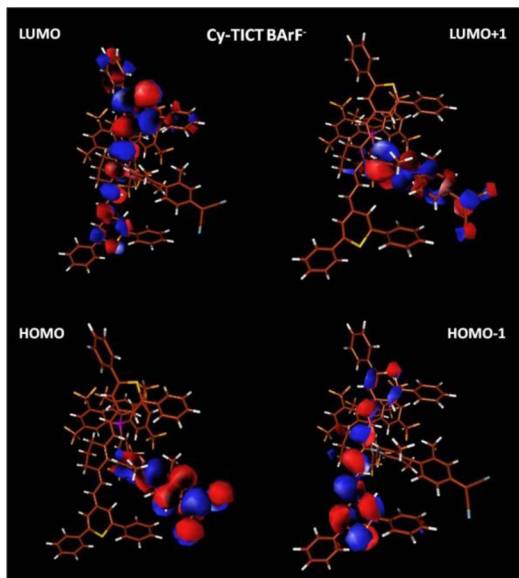


Figure 4. Cy-TICT frontier molecular orbitals computed at the DFT CAM-B3LYP/6-31G(d,p) level.

In summary, we show both experimentally and theoretically that coupling a twisted π -electron motif to a cyanine dye results in significant enhancement of both the real and imaginary parts of the second hyperpolarizability and, consequently, of the intensity-dependent refractive index and two-photon absorbance cross-section. New chromophore Cy-TICT shows a third-order NLO response, substantially exceeding the combined contributions of the parent dyes. We attribute this cooperative enhancement to cross-coupling between the closely spaced twisted chromophore zwitterionic and cyanine states and to a simultaneous fall in the cyanine bond length alternation parameter.

■ ASSOCIATED CONTENT

📄 Supporting Information

Experimental details, characterization data for new compounds, and additional results. This material is available free of charge via the Internet at <http://pubs.acs.org>.

■ AUTHOR INFORMATION

Corresponding Authors

*pnprasad@buffalo.edu

*t-marks@northwestern.edu

Notes

The authors declare no competing financial interests.

■ ACKNOWLEDGMENTS

This work was supported by AFSOR Grant FA-95500610398 and MURI grant FA-95501410040. A.J.-T.L. thanks NDSEG for a Graduate Research Fellowship.

■ REFERENCES

- (1) (a) Samoć, M. *J. Mol. Model.* **2011**, *17*, 2183. (b) Pawlicki, M.; Collins, H. A.; Denning, R. G.; Anderson, H. L. *Angew. Chem., Int. Ed.* **2009**, *48*, 3244. (c) He, G. S.; Tan, L.-S.; Zheng, Q.; Prasad, P. N. *Chem. Rev.* **2008**, *108*, 1245.
- (2) (a) Huang, C.; Sartin, M. M.; Siegel, N.; Cozzuol, M.; Zhang, Y. D.; Hales, J. M.; Barlow, S.; Perry, J. W.; Marder, S. R. *J. Mater. Chem.* **2011**, *21*, 16119. (b) He, G. S.; Zheng, Q.; Prasad, P. N.; Helgeson, R.; Wudl, F. *Appl. Opt.* **2005**, *44*, 3560. (c) Lin, T.-C.; He, G. S.; Prasad, P. N.; Tan, L.-S. *Opt. Lett.* **2004**, *14*, 982. (d) Norman, P.; Luo, Y.; Ågren, H. *J. Chem. Phys.* **1999**, *111*, 7758.
- (3) (a) Thorley, L. J.; Hales, J. M.; Anderson, H. L.; Perry, J. W. *Angew. Chem., Int. Ed.* **2008**, *47*, 7095. (b) de La Torre, G.; Vázquez, P.; Agulló-López, F.; Torres, T. *Chem. Rev.* **2004**, *104*, 3725. (c) Marder, S. R.; Torruellas, W. E.; Blanchard-Desce, M.; Ricci, V.; Stegeman, G. I.; Gilmour, S.; Brédas, J.-L.; Li, J.; Bublitz, G. U.; Boxer, S. G. *B. Science* **1997**, *276*, 1233.
- (4) Prasad, P. N.; Williams, D. J. *Nonlinear Optical Effects in Organic Molecules and Polymers*; John-Wiley & Sons, Inc.: New York, 1991.
- (5) (a) Isborn, C. M.; Leclercq, A.; Vila, F. D.; Dalton, L. R.; Brédas, J.-L.; Eichinger, B. E.; Robinson, B. H. *J. Phys. Chem. A* **2007**, *111*, 1319. (b) Marder, S. R.; Beratan, D. N.; Cheng, L.-T. *Science* **1991**, *252*, 103. (c) Oudar, J. L.; Chemla, D. S. *J. Phys. Chem.* **1977**, *66*, 2664.
- (6) Meyers, F.; Marder, S. R.; Pierce, B. M.; Brédas, J.-L. *J. Am. Chem. Soc.* **1994**, *116*, 10703.
- (7) Murugan, A. N.; Kongsted, J.; Rinkevicius, Z.; Ågren, H. *Proc. Natl. Acad. Sci. U.S.A.* **2010**, *107*, 16453.
- (8) (a) Kang, H.; Facchetti, A.; Jiang, H.; Cariati, E.; Righetto, S.; Ugo, R.; Zuccaccia, C.; Macchioni, A.; Stern, C. L.; Liu, Z. F.; Ho, S. T.; Brown, E. C.; Ratner, M. A.; Marks, T. J. *J. Am. Chem. Soc.* **2007**, *129*, 3267. (b) Brown, E. C.; Marks, T. J.; Ratner, M. A. *J. Phys. Chem. B* **2008**, *112*, 4. (c) Albert, I. D. L.; Marks, T. J.; Ratner, M. A. *J. Am. Chem. Soc.* **1998**, *120*, 11174.
- (9) He, G. S.; Zhu, J.; Baev, A.; Samoć, M.; Frattarelli, D. L.; Watanabe, N.; Facchetti, A.; Ågren, H.; Marks, T. J.; Prasad, P. N. *J. Am. Chem. Soc.* **2011**, *133*, 6675.
- (10) (a) Kang, H.; Facchetti, A.; Stern, C. L.; Rheingold, A. L.; Kassel, W. S.; Marks, T. J. *Org. Lett.* **2005**, *7*, 3721. (b) Yin, J.; Rainka, M. P.; Zhang, X.-X.; Buchwald, S. L. *J. Am. Chem. Soc.* **2002**, *124*, 1162.
- (11) (a) Li, Z.; Liu, Y.; Kim, H.; Hales, J. M.; Jang, S. H.; Luo, J. D.; Baehr-Jones, T.; Hochberg, M.; Marder, S. R.; Perry, J. W.; Jen, A. K. *Adv. Mater.* **2012**, *2012*, OP326. (b) Hales, J. M.; Matichak, J.; Barlow, S.; Ohira, S.; Yesudas, K.; Brédas, J.-L.; Perry, J. W.; Marder, S. R. *Science* **2010**, *327*, 1485. (c) Hales, J. M.; Barlow, S.; Kim, H.; Mukhopadhyay, S.; Brédas, J.-L.; Perry, J. W.; Marder, S. R. *Chem. Mater.* **2014**, *26*, 549.
- (12) For crystallographic characterization of related molecules, see: Nagao, Y.; Sakai, T.; Kozawa, K.; T. Urano, T. *Dyes Pigm.* **2007**, *73*, 344 and references therein.
- (13) Milam, D. *Appl. Opt.* **1998**, *37*, 546.
- (14) He, G. S.; Zheng, Q.; Baev, A.; Prasad, P. N. *J. Appl. Phys.* **2007**, *101*, 0831081.
- (15) DALTON, a molecular electronic structure program. <http://daltonprogram.org/>, 2011.
- (16) (a) Del Zoppo, M.; Castiglioni, C.; Gerola, V.; Zuliani, P.; Zerbi, G. *J. Opt. Soc. Am. B* **1998**, *15*, 308. (b) Ohira, S.; Hales, J. M.; Thorley, K. J.; Anderson, H. L.; Perry, J. W.; Brédas, J.-L. *J. Am. Chem. Soc.* **2009**, *131*, 6099. (c) Bartkowiak, W.; Zaleśny, R.; Leszczynski, J. *Chem. Phys.* **2003**, *287*, 103.